Syntheses of Silver Nanoparticles in the Matrices of Block Copolymers in Aqueous Solutions

S.V. Fedorchuk[1,*], T.B. Zheltonozhskaya[1,†], Yu.P. Gomza[2], S.D. Nessin[2,‡], L.R. Kunitskaya[1,§]

[1] *Kiev National Taras Shevchenko University, Faculty of Chemistry, Department of Macromolecular Chemistry, 60 Vladimirskaya St, 01033 Kiev, Ukraine*
[2] *Institute for Macromolecular Chemistry, National Academy of Sciences of Ukraine, 48 Kharkovskoye Shosse, 02160 Kiev, Ukraine*

In the present work we have synthesized two-component block copolymers MOPEO-*b*-PAAm and PAAm-*b*-PEO-*b*-PAAm comprised methoxypoly(ethylene oxide), poly(ethylene oxide) and chemically complementary polyacrylamide. These copolymers we used as special matrices in the process of borohydride reduction of Ag+ ions. It was established the influence of chemical nature, molecular architecture and concentration of the matrices and the content of silver nitrate on some reaction parameters, size and stability of Ag-nanoparticles in aqueous solutions.

Keywords: Nanoparticles, Matrix, Self-assembly, Supramolecular structures, X-ray scattering.

PACS numbers: 82.35.Jk, 61.46.Df

1. INTRODUCTION

One of the actual aspects of the nanotechnology development is elaboration of the controlled synthesis methods of metal nanoparticles, which are active components of nanoscale electronics, photonics and sensorics. The metal solutions, mainly gold, silver and platinum group metal, intensive were studied in the last century. Although the synthesis and the physical characterization of metal nanocrystals have been generally investigated, considerably less attention has been devoted to the fabrication of novel nanostructured materials. However, the high chemical activity of zero-valent metals can cause the irreversible aggregation of the nanoparticles that creates the problem of their storage stability. In order to solve this problem, the development of the nanoparticle synthesis methods in polymer matrices, which will ensure the control of nanoparticle sizes, forms and stabilization in a solution, is necessary. At the last time, the amphiphilic block copolymers, which form micellar structures, are used to obtain the Ag-containing nanosystems mainly in organic medium. However, in separate cases (for example, at the use of silver nanoparticles in medicine and catalysis of chemical reactions) the nanoparticles should be obtained and stabilized in a hydrophilic environment.

In the present work, we synthesized the IntraPC-forming triblock copolymers (TBCs) such as PAAm-*b*-PEO-*b*-PAAm with hydrophilic biocompatible and partially biodegradable blocks of poly(ethylene oxide) and polyacrylamide of a variable length. Then we studied their micellization in aqueous and aqueous/ethanol solutions and encapsulation of a model poorly soluble drug prednisolon (PS) into the micellar nanocontainers.

2. EXPERIMENTAL

2.1 Materials and syntheses

We carried out syntheses of MOPEO-*b*-PAAm diblock copolymer (DBC) and PAAm-*b*-PEO-*b*-PAAm triblock copolymer (TBC) using the template radical block and graft copolymerization, which was initiated by the Red/Ox reaction of cerium ammonium nitrate with hydroxyl groups of MOPEG and PEG [1,2].

The reagents were mixed in the deionized water and inert atmosphere at 25 °C for 24 h. The molar ratios $[Ce^{IV}]/[PEG] = 2$ and $[Ce^{IV}]/[AAm] = 1 \cdot 10^{-3}$ were constant in all cases. Gel-like TBCs were diluted by water, re-precipitated by acetone, dissolved again in water and freeze-dried. The molecular weights of PAAm blocks in DBC and TBC ($M_{nPAAm} = 29.8$ and 117.0 kDa, respectively) were determined by NMR spectroscopy [3].

The reduction of silver ions was carried out in aqueous polymer solutions with the eightfold molar excess of $NaBH_4$ that allowed achieving practically complete conversion of Ag+ ions to zero-valent state in a selected region of $AgNO_3$ concentrations ($C_{AgNO_3} = 0.91 \cdot 10^{-2}$ and $1.82 \cdot 10^{-2}$ kg·m^{-3}) [4]. According to the studies [5], the process of Ag+-ion reduction can be represented by the total stochiometric equation:

$$8Ag^+ + BH_4^- + 8OH^- = 8Ag + H_2BO_3^- + 5H_2O$$
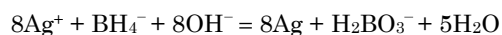
At the same time, borohydride anions participate also in some side reactions, due to which their essential excess is used to enhance the yield of Ag nanoparticles [4].

Polymeric solutions was mixed with $AgNO_3$ and kept for 30 min in a dark box; then the reducing agent was added. We varied concentrations of the polymeric matrices ($C_m = 0.5$, 1.0 and 2.0 kg·m^{-3}) and silver salt (see above).

* sergey_fedorchuk@ukr.net
† zheltonozhskaya@ukr.net
‡ polymer7@ukr.net
§ larisa_kunitskaya@ukr.net

2.2 Characterization

The process of nanoparticle formation was controlled by the changes in the position (λ_{max}) and the integral intensity (S) of the surface plasmon resonance band (SPRB), which was displayed in a visible region of spectrum [4,6]. The time evolution of the extinction spectra was recorded in a three-minute interval in a region of 200-1000 nm using a Cary 50 Scan UV-Vis spectrometer from "Varian" (USA).

WAXS profiles for the dried compositions were obtained in a cell with a thickness of 2 mm using a DRON-2.0 X-ray difractometer with Ni-filter in a primary beam. The monochromatic Cu-K$_\alpha$ radiation with $\lambda = 0.154$ nm, filtered by Ni, was provided by an IRIS M7 generator (at operating voltage of 30 kV and a current of 30 mA). The scattered intensities were measured by a scintillation detector scanning in 0.2° steps over the range of the $\theta = 3$-45° scattering angles (corresponding to $q = 2.13$-31.21 nm^{-1}, where $q = 4\pi \cdot sin(\theta/2)/\lambda$ is the wavevector or the scattering vector). The diffraction curves obtained were reduced to equal intensities of the primary beam and equal values of the scattering volume [7]. Also, the normalization of experimental scattered intensities was carried out according to the formula:

$$I_{n(i)}(\theta) = \left[I_{\exp}(\theta) - I_b(\theta) \right] \cdot (I/I_0)$$

where $I_{exp}(\theta)$ and $I_{n(i)}(\theta)$ are the experimental and normalized intensities in WAXS profile as a function of θ, $I_b(\theta)$ is the intensity of the background for every θ value, I_0 and I are the intensities of incident and scattered beams at $\theta = 0°$ (the coefficient of the beam weakening).

SAXS profiles for the compositions were obtained in an automated Kratky slit-collimated camera. Here copper anode emission monochromated by total internal reflection and nickel filter was used. The intensity curves were recorded in the step-scanning mode of the scintillation detector in a region of the $\theta = 0.03$-4.0° scattering angles (the wavevector $q = 0.022$-2.86 nm^{-1}). Thus, the study of the micro-scale heterogeneous domains with characteristic dimensions (evaluated as $2\pi/q$) from 2 to 280 nm was possible. Normalization of SAXS profiles was carried out using the FFSAXS-3 program [7] and a standard sample from the laboratory of professor Kratky. The scattered intensities were normalized to the sample thickness and the scattered intensity of a standard. Additionally, the raw intensity curves were smoothed, corrected for parasitic scattering and desmeared.

3. RESULTS AND DISCUSSION

The state of DBC, TBC, PVA-g-PAAm and SiO$_2$-g-PAAm in aqueous solutions was considered in our previous publications It was shown [1,8] that asymmetric macromolecules of DBC and TBC formed the "hairy-type" micelles in aqueous medium due to interaction of MOPEO (PEO) and PAAm blocks followed by segregation (self-assembly) of non-polar bound parts. Stability of DBC and TBC micelles, which was evaluated by both the critical micellization concentration and the Gibbs free micellization energy ($CMC = 1.3 \cdot 10^{-5}$ and $0.37 \cdot 10^{-5}$ mol·dm^{-3}; -$\Delta G = 32.98$ and 36.15, kJ·mol^{-1}, consequent-

ly), turned out to be higher for TBC. Relatively small "core" of these micelles contained non-polar bound parts of both the blocks but the developed "corona" comprised the segments of longer PAAm chains, which were unbound with PEO.

3.1 Kinetics and products of borohydride reduction of silver ions

In 3-5 minutes after addition of the reducing agent to the mixtures of DBC, TBC, with AgNO$_3$, a yellow coloring, which corresponded to the color of the diluted silver nanodispersions in water [4,6], was appeared. The coloring intensity increased for 1-3 h at $C_{AgNO3} = 1.82 \cdot 10^{-2}$ kg·m^{-3}. But at lower concentrations of silver ions ($C_{AgNO3} = 0.91 \cdot 10^{-2}$ kg·m^{-3}) and at $C_m = 0.5$ and 1.0 kg·m^{-3}, a yellow color was quickly disappeared and a black precipitate arose. The same picture was observed in the case of Ag+-ion reduction in polymer-free solutions with low concentration of AgNO$_3$. The results for 90 min, which were obtained at the maximum concentrations of the matrices and AgNO$_3$, are shown in Fig. 1:
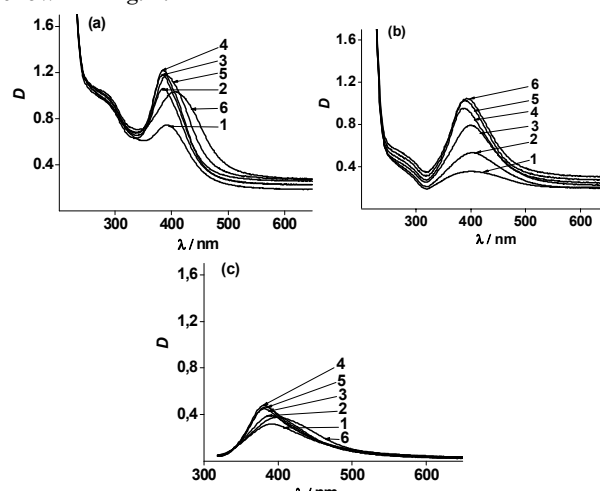
Fig. 1 – The time evolution of the absorption spectra in aqueous blends of (**a**) MEPEO-b-PAAm, (**b**) PAAm-b-PEO-b-PAAm and (**c**) refers to the same reaction in the polymer-free solution with AgNO$_3$ in 5 -*1*, 15 -*2*, 21 -*3*, 36 -*4*, 60 −*5* and 90 min −*6* after NaBH$_4$ introduction. $C_m = 2.0$ kg·m^{-3}, $C_{AgNO3} = 1.82 \cdot 10^{-2}$ kg·m^{-3}

The formation of spherical Ag nanoparticles much smaller than the wavelength of light results in the appearance of a single narrow SPRB with $\lambda_{max} = 380$-425 nm in the extinction spectra [6,9]. Exactly such Ag nanoparticles formed in the studied reaction blends that was confirmed by a unimodal narrow SPRB ($\lambda_{max} = 379$-400 nm), which was observed in all the spectra. At the same time, in DBC solutions and also in polymer-free solutions, such effects as SPRB widening in time and a red shift of λ_{max} were also revealed (Fig. 1 a, c). In principal, there are some reasons, which could initiate the last effects [9]: i) increase in a size (or polydispersity) of spherical Ag nanoparticles, ii) formation more stretched Ag particles (spheroids, ellipsoids etc.), and iii) aggregation of Ag nanoparticles. But taking into account the presence in the spectra (Fig. 1 a, c) only a single SPRB, we achieved the important conclusion

about a small value of all proposed alterations in the above-mentioned systems. Indeed, in the case of a large increase in the Ag nanoparticle size, an additional (quadrupole) SPRB would appear in the spectrum. Analogous picture would observe, when strongly stretched Ag nanoparticles with a large aspect ratio or the developed aggregates of nanoparticles appear.

Note, that the Ag+-ion reduction was also occurred at the pointed C_{AgNO3} in polymer-free solutions (Figure 1**c**) but the yield of nanoparticles, which could be evaluated by the integral intensity S of SPRB (see discussion above), was less as compared to that in polymeric solutions. Similar results were obtained in the study[10] and explained by a small stabilizing action of Ag+ ions adsorbed on the surface of growing nanoparticles. But at lower C_{AgNO3}, the formation of stable enough Ag nanoparticles was not observed.

The spectra of all the reaction blends in Fig. 1 demonstrated additionally a weak band in the region of $\lambda \sim 270\text{-}290$ nm. This absorption band is known to reflect the presence of the charged Ag_4^{2+} nanoclusters [9], which arise at the initial stage of silver reduction. The maximum intensity of the band was observed in DBC solutions (Fig. 1 a).

3.2 Structure of polymeric compositions with silver nanoparticles

The bulk structure of some polymer-metal compositions was characterized and the size of Ag nanoparticles was determined using wide-angle and small-angle X-ray scattering (WAXS and SAXS). The polymer-metal compositions were cast from aqueous solutions ($C_m = 2.0$ and $C_{AgNO3} = 3.64$ kg·m⁻³) into special Teflon forms placed in a dark box and then were dried on air and in a vacuum desiccator for 10 days. The results (Fig. 2) showed that the bulk structure of the compositions contained a polymeric amorphous phase, that was displayed in WAXS profiles by two diffusive overlapped maxima at $\theta \sim 15°$ and $21°$, and crystalline Ag nanoparticles, that was confirmed by characteristic crystalline peaks of silver (111) at $\theta \sim 38°$[11]. The appearance of these peaks indicated the formation of crystalline Ag nanoparticles with tetragonal facet-centered cubic lattice [11]. An amorphous character of polymeric phases in the compositions was completely correlated with the data of DSC studies [3,12], which demonstrated the loss of PEO crystalline properties in the block copolymer structure because of the interaction of the main and grafted chains.
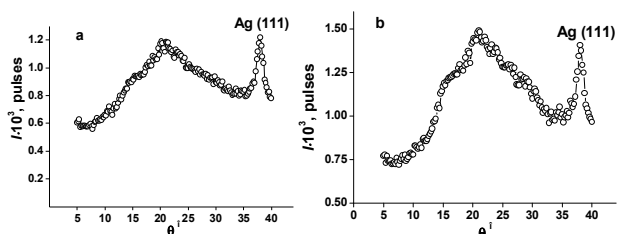
Fig. 2 – WAXS difractograms for the compositions: (a) ME-PEO-*b*-PAAm+Ag and (**b**) PAAm-*b*-PEO-*b*-PAAm+Ag. $T = 20$ °C.

As to the presence of two diffusive overlapped maxima in WAXS profiles in Fig. 2, they could be attributed (as in the study [12]) to the presence of two systems of planes of the paracrystalline lattice [38] in the amorphous regions of PAAm-*b*-PEO-*b*-PAAm and MEPEO-*b*-PAAm structures, which contain mainly PAAm chains. The first maximum with smaller intensity at $\theta \sim 15°$ characterizes the lateral periodicity in an arrangement of PAAm chains but the second one with greater intensity at $\theta \sim 21°$ reflects the periodic arrangement of the flat hydrogen-bonded *cis*-dimers of amide groups in the structures of *cis-trans*-multimers [1].

The results in a form of the dependences of the scattered intensities versus q are shown in Fig. 3.
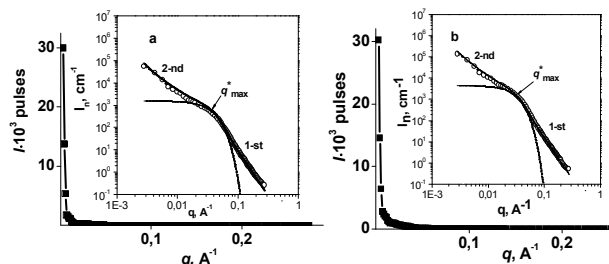
Fig. 3 – The intensity of small-angle X-ray scattering *vs* the wavevector for the compositions: (**a**) MEPEO-*b*-PAAm +Ag and (**b**) PAAm-*b*-PEO-*b*-PAAm +Ag. The double logarithmic SAXS profiles are shown in a lesser scale; ○ (**a**) = MEPEO-*b*-PAAm +Ag, ○ (**b**) = PAAm-*b*-PEO-*b*-PAAm +Ag.

All the profiles demonstrated a sharp fall in the scattered intensities with q growth (without any diffraction maxima) that pointed out the absence of any periodicity in the arrangement of structural elements of the compositions and polymer-inorganic hybrid at the supramolecular level. The same profiles in two logarithmic coordinates are exhibited in Fig. 3 in a lesser scale. Let's carry out their analysis from the point of view the fractal-cluster organization of the composition structure [13].

The double logarithmic SAXS profiles for the both compositions demonstrated two linear parts with different slopes, which corresponded to two power scattering regimes by Porod ($I \approx q^{-Df}$, where D_f is the slope ratio for corresponding straight line of log I *vs* log q). These linear parts were connected by the curve, which conformed to the exponential scattering regime by Guinier [13]. Such form of SAXS profiles in the double logarithmic coordinates pointed out the two-level fractal organization of a bulk structure of the compositions and polymer-inorganic hybrid. The character of separate elements of each level (the mass-fractal clusters, the surface-fractal clusters or solid particles with a smooth surface) could be determined by analysis of D_f value but the maximum diameter of these elements could be estimated by the relation $d_{max} \sim 2\pi/q^*$[7,13]. Finding the last parameter is possible in the case, when the straight line corresponding to the power scattering regime by Porod is ended (or "cuts") by the scattering regime by Guinier in the region of small q that is when a separate structural level is clearly displayed. A definite q^* value, which is determined in the region of the Guinier's scattering (Fig. 3) [13], is considered as "the cutting border". All said parameters (D_f, q^* and d_{max}) were established only for the 1-st lower level of structural organization of the compositions, which was displayed at higher q. For the 2-nd higher structural

level, which was revealed at less q, only D_f numbers were found (Table 1) because corresponding straight lines of the Porod's scattering in Fig. 3 were not restricted from above by the Guinier's scattering regimes.

It is well known [13], that the $D_f = 4$ value characterizes the power scattering regime by Porod in the case of the dense solid scattering particles with a smooth surface. Exactly such values were determined for the linear parts of SAXS profiles, which corresponded to the 1-st structural level of the compositions (Table 1). This fact additionally confirmed the formation of the dense Ag nanoparticles in both the polymeric matrices. The maximum radius of a gyration for these particles was calculated using d_{max} value and the relation: $[R_g = d_{max}/2(5/3)^{1/2}]$ [13]. It turns out to be essentially less in the composition with MEPEO-*b*-PAAm (Table 1). Thus, the dense crystalline Ag nanoparticles constituted the 1-st level of the fractal-organized structure of the polymer-metal composites.

Table 1

System / Value	MEPEO-*b*-PAAm		PAAm-*b*-PEO-*b*-PAAm	
	1-st	2-nd	1-st	2-nd
D_f	4.0	2.2	3.9	2.2
$q^* \cdot 10^2$ / A^{-1}	3,9	-	2,8	-
d_{max} / nm	16,2	-	22,4	-
R_g / nm	6,3	-	8,7	-
R_g (calc) / nm	5,0	-	6,0	-

The computer modeling of SAXS profiles by the method of global unified exponential-power functions, which was designed by Beaucage with co-workers [14], is actively used in the studies of fractal-organized polymeric and composition materials [13,14]. These authors showed that the double logarithmic SAXS profiles for fractal-organized materials could contain two or more power regimes. Their approach consisted in the separation of several structural levels (in accordance with the number of the power scattering regimes), which were limited from above by the exponential scattering regimes by Guinier, and consideration of separate contributions from each structured level to the total scattering function. The equation describes the

arbitrary number of interrelated structural levels [13,14]:

$$I(q) = \sum_{i=1}^{n} (G_i \exp\left(-q^2 R_{g_i}^2 \big/ 3\right) + B_i \exp\left(-q^2 R_{g_{(i+1)}}^2 \big/ 3\right) \times$$
$$\times \left\{ \left[erf\left(qR_{g_i} \big/ 6^{1/2} \right) \right]^3 \big/ q \right\}^{P_i})$$

Here G_i is the coefficient of Guinier's relation for i-level; B_i is the coefficient of Porod's term for the same level; D_f is the slope ratio for the power dependence of log I versus log q, which one defines the fractal dimension of the aggregates by i-level (for the surface fractals $-4 < D_f < -3$ while for the mass fractals $D_f > -3$); R_g is the radius of a gyration for the fractal aggregates by i-level.

Using Beaucage's method, we modeled SAXS profiles for both the compositions taking into consideration two levels of their structural organization, which were discussed above. The $R_{g(calc)}$ values, which were calculated by Beaucage's approach for: i) Ag nanoparticles in the composition structure and ii) the surface-fractal clusters with "cores" these micelles which consist of non-polar bound parts of both the blocks but the developed "corona" comprised the segments of longer PAAm chains, which were unbound with PEO.

4. CONCLUSION

Thus, the block copolymers PAAm-*b*-PEO-*b*-PAAm and MEPEO-*b*-PAAm, which form IntraPCs and self-assemble in micellar structures in aqueous solutions, could be considered as efficient nanoreactors. They are capable of ensuring the high rate and efficacy of the borohydride reduction of silver ions up to the stable crystalline Ag nanoparticles with $R_g \sim$ 5-6 nm. The compositions of PAAm-*b*-PEO-*b*-PAAm and MEPEO-*b*-PAAm with Ag nanoparticles showed the two-level fractal organization of their structure. The dense crystalline silver nanoparticles were the separate elements of the 1-st lower level, while the mass-fractal clusters of the polymeric matrices constituted the 2-nd higher structural level.

REFERENCES

1. T Zheltonozhskaya, N Permyakova, L Momot, in: "*Hydrogen-Bonded Interpolymer Complexes. Formation, Structure and Applications*" Ch.5, V.V. Khutoryanskiy, G. Staikos (New Jersey-London-Singapore-Beijing etc.: World Scientific, 2009).
2. T.B .Zheltonozhskaya, S.V. Fedorchuk, V.G. Syromyatnikov. *Russ. Chem. Rev.* **76**, 731 (2007**)**.
3. S.V. Fedorchuk,T.B. Zheltonozhskaya, E.M. Shembel, L.R. Kunitskaya, I.M. Maksuta, Y.P. Gomza, *Functional materials*. **18**, 1 (2011).
4. B. Sergeev, L. Lopatina, A.Prusov, G. Sergeev, *Colloid. J.* **67**, 79 (2005).
5. Maltceva N.N., Hain V.S., "*Sodium borohydride. Characteristic and application*" (Nauka, Moscow, 1985).
6. S. Horikoshi, H. Abe, K. Torigoe, M. Abe, Nick. Serpone, *Nanoscale* **2**, 1441 (2010).
7. Yu.S.Lipatov, V.V.Shilov, Yu.P.Gomza et al. "*X-Ray Diffraction Methods to Study Polymeric Systems*" (Nauk. Dumka, Kyiv, 1982).
8. L.R. Kunitskaya, V.A. Aleinichenko, T.B. Zheltonozhskaya, S.A. Berkova, *Mat.-wiss. u. Werkstofftech.* **42**, 109 (2010).
9. A. Henglein *J. Phys. Chem.* **97**, 5457 (1993).
10. D. G. Angelescu, M. Vasilescu, R. Somoghi, D. Donescu, V. S. Teodorescu, *Colloids and Surfaces A: Physicochem Eng. Asp.* **366**, 155 (2010).
11. Becturov E.A., Kudaybergenov S.E., Garmagambetova A.К., Iskakov R.M., Ibraeva J.E., Shmakov S.N. "*Polymer-protected metal nanoparticles*" (Almaty, 2010).
12. S. Fedorchuk, T.Zheltonozhskaya, N. Permyakova, Y. Gomza, S. Nessin, V. Klepko, *Mol. Cryst. Liq. Cryst.* **497**, 268 (2008).
13. A.P. Shpak, V.V. Shilov, O.A. Shilova, Yu.A. Kunitskiy, "*Diagnostics of nanosystems. Multilevel fractal structures*" (Nauk. Dumka, Kyiv, 2004).
14. G. Beaucage, J. Hyeonlee, Se. Pratsinis, S. Vemury, *Langmuir* **14**, 5751 (1998).